

Non-stochastic Optimization Algorithm for Neural-network Quantum States

Xiang Li¹, Jia-Cheng Huang¹, Guang-Ze Zhang¹, Changsu Cao^{1,2}, Han-Shi Hu^{1,*}

¹*Department of Chemistry and Engineering Research Center of Advanced Rare-Earth Materials of Ministry of Education, Tsinghua University, Beijing 100084, China*

²*ByteDance Research, Zhonghang Plaza, No. 43, North 3rd Ring West Road, Haidian District, Beijing, 100089, China*

(Dated: March 2023)

Neural-network quantum states (NQS), which use an artificial neural network to encode variational many-body wave functions in second quantization, have been successfully applied to the electronic problem for several molecules recently. Though already competes with many traditional quantum chemistry methods, describing electronic wave function of molecules using NQS is just in its early stages. Here we introduce a general non-stochastic optimization algorithm for NQS in chemical systems, which deterministically generates a selected set of important configurations simultaneously with energy evaluation of NQS and sidesteps Markov-chain Monte Carlo that is required in the typical variational Monte Carlo (VMC) framework, making the whole optimization smoother and faster. This newly developed non-stochastic optimization algorithm for NQS can recover the potential energy curves with a level of accuracy competitive with CCSD(T) in carbon dimer with cc-pVDZ basis after perturbative correction with $\sim 1.4 \times 10^{11}$ configurations in the full variational space, and to an accuracy of better than 0.2 mHa in strongly correlated equidistant hydrogen chain H_{10} with STO-6G basis. These successful applications of NQS to molecules that have large variational spaces or strong electron correlations manifest the strength of our non-stochastic optimization algorithm, provide further understanding about the performance of NQS in chemical systems and suggest routes for future improvements.

1. INTRODUCTION

The search for solutions of the many-electron Schrödinger equation is one of the substantial problems in modern electronic structure theory. In the context of ab initio quantum chemistry, it is particularly convenient to solve for the electronic wave functions on the basis of Slater determinants.

The exact approach is full configuration interaction (FCI) method considering all electron configurations but is limited to small molecules. Although various methods based on different representations of many-electron wave functions have been developed to approximate the FCI ground states, there are limitations in these methods directly or indirectly arising from the choice of wave function approximation or ansatz, which is a trade-off between efficiency and accuracy. For example, the coupled cluster (CC) methods^{1, 2} can accurately and efficiently treat chemical systems with clear hierarchy but perform relatively poorly when confronted with strong static correlations or multi-reference problems. One natural proposal to this challenge is employing the complete active space (CAS) methods^{3, 4}, which build up a multi-determinantal wave function using all possible determinants within the active space. However, applications of CAS methods or other multireference theories^{5, 6} are limited to a relatively small number of active electrons and orbitals. Even though another advanced method named density matrix renormalization group⁷ (DMRG) is applicable to large active spaces and is extremely efficient in describing molecules that are quasi-one-dimensional, it also suffers from its variational form, the matrix product states⁸ (MPS), because high-dimensional systems require more general tensor-network states^{9, 10}.

The common strategy of most quantum chemical methods for constructing wave function ansatz that can efficiently approximate the FCI wave function is reducing the exponential complexity of FCI wave function down to its most essential features. One prime example is selected configuration interaction (SCI) methods¹¹⁻¹⁹, which capitalizes on the paucity of configurations that contribute appreciably to the exact wave function and tackle large active spaces by iteratively augmenting a selected set of those important determinants as follows. At each iteration, all of the determinants connected to any selected determinant by Hamiltonian matrix elements that have a nonzero or sufficiently large amplitude are examined, and only important determinants are selected. The resultant multi-determinantal variational wave function can capture much of the accuracy of FCI but using a small fraction of all possible configurations. The minor deficiency is just the memory bottleneck comes from storing the Hamiltonian matrix in variational space¹⁶. Besides, the variational energy can be further improved by employing a second-order perturbative correction using multireference Epstein-Nesbet perturbation theory^{20, 21}, which is known as selected configuration interaction plus perturbation theory (SCI+PT) methods.

This strategy for tackling the exponential scaling of FCI wave function resembles dimensional reduction and feature extraction in data science²², suggesting the possibility of leveraging the power of artificial neural networks (ANN) to help overcome some of the limitations of existing wave function ansatz. In 2017, Carleo and Troyer first introduced an ANN model based on the restricted

Boltzmann machine (RBM) to compactly encode the many-body wave function with high precision in discrete spin lattice systems, and referred to this type of wave function ansatz as neural-network quantum states²³ (NQS). The reinforcement learning scheme on the basis of energy minimization proposed in their seminal work employs the Monte Carlo (MC) sampling to calculate expectation values and is an ab initio and variational approach that requires no pre-existing data nor prior knowledge of the exact wave function to train the neural network and has no fundamental limits to its accuracy. This innovative idea is then extended to approximate the fermionic wave function of chemical molecules in second-quantized form²⁴⁻²⁷ or in continuous space²⁸⁻³⁰ and many other more recent applications are summarized³¹. In discrete basis, NQS is served as a function of the unique occupation number representation of different electron configurations to parametrize their coefficients, which is motivated by the fact that neural networks are universal function approximators. Even though the introduced RBM is a relatively simple shallow neural network, it is able to capture most of the accuracy of FCI on several model molecules²⁴. This impressive performance can be partly explained by the intimate connection between RBM and two-dimensional tensor network³²⁻³⁴. Furthermore, several extensions of RBM-based NQS were demonstrated to yield a promising improvement³⁵⁻³⁷. However, there are still challenges in applying the NQS to large chemical systems mainly originated from the inherent MC sampling procedures. The first is the inefficiency of MC sampling when dealing with the peculiar structure of molecular ground-state wave function, which is typically sharply peaked around the Hartree-Fock state and neighboring excited states²⁴. A way to circumvent this limitation is proposed recently but only applicable with the autoregressive models³⁸⁻⁴⁰. Another challenge is related to the statistical error resulting from MC sampling, which is proportional to the inverse square root of the number of sampling points used^{41,42}. Thus the noise introduced by stochastic optimization with MC sampling would get worse when calculating small energy differences³¹.

To address these two challenges involved with MC sampling, in this article, we first incorporate the cardinal idea of SCI methods into a new non-stochastic optimization algorithm for NQS, in which a set of important configurations that have relatively large probabilities is deterministically selected simultaneously with the energy evaluation of NQS. This deterministically selected set of important configurations can serve as a substitute of the MC configuration sample required in the stochastic NQS optimization, because the MC sample is likewise a set of important configurations that have relatively large probabilities though generated stochastically. In addition, integrating the configuration selection into energy evaluation removes the significant computational bottleneck that stems from MC sampling. Finally, we make an attempt to exploit the perturbation theory to

correct the variational energy of NQS in two different schemes, yielding a notable refinement of the energy accuracy.

The rest of this paper is organized as follows. In section 2, we briefly recapitulate the basics of RBM-based NQS and the unsupervised, variational, and stochastic optimization algorithm which requires MC sampling. In section 3, we describe the details of our new non-stochastic optimization algorithm, and the two approaches to apply perturbation theory. Next, in section 4, we compare our non-stochastic algorithm with the stochastic algorithm in accuracy and efficiency, and then benchmark the accuracy of RBM-based NQS with non-stochastic algorithm against FCI results by applying it to carbon dimer with both STO-3G and cc-pVDZ basis, and equidistant linear hydrogen chain H_{10} with STO-6G basis. Finally, section 5 gives the conclusions.

2. NEURAL-NETWORK QUANTUM STATES

2.1. Representation of Many-electron Wave Functions. The basic idea of neural-network quantum states is to encode the many-body wave function in a second-quantized form using one flexible neural network, such as the complex-valued, shallow restricted Boltzmann machine. When apply the NQS to quantum chemistry, we consider the many-electron wave function on the basis of Slater determinants

$$|\Psi_\theta\rangle = \sum_{\sigma_1, \sigma_2, \dots, \sigma_M} C_{\sigma_1, \sigma_2, \dots, \sigma_M} \times |\sigma_1, \sigma_2, \dots, \sigma_M\rangle = \sum_i \langle D_i | \Psi_\theta \rangle \times |D_i\rangle, \quad (1)$$

where $|D_i\rangle = |\sigma_1, \sigma_2, \dots, \sigma_M\rangle$ is one electron configuration in Slater determinant form, $\sigma_i \in \{0, 1\}$ is the occupation number of each electronic spin orbital and M is the number of electronic spin orbitals. It is obvious that one artificial neural-network with parameters θ can be used to describe $C_{\sigma_1, \sigma_2, \dots, \sigma_M}$, the coefficients of each configuration. Here, we specialize our discussion to the RBM architectures, which have been successfully used in a variety of interacting quantum models^{23, 33, 36, 43-47} and several chemical molecules^{24, 25}. In this work, we describe RBM wave function ansatz using the compact form

$$C_{\sigma_1, \sigma_2, \dots, \sigma_M} = \langle D_i | \Psi_\theta \rangle = e^{\sum_i a_i \sigma_i} \prod_j^{[\alpha \cdot M]} \left(1 + e^{b_j + \sum_i^M w_{ij} \sigma_i} \right), \quad (2)$$

where $\theta = \{a, b, W\}$ is a set of complex-valued network parameters and the hidden unit density α determines the expressive power of this formula.

2.2. Optimization of Neural-network Quantum States using Monte Carlo. The NQS wave function ansatz is typically optimized through a variational approach known as variational Monte Carlo (VMC), by minimizing its energy expectation value

$$E_\theta = \frac{\langle \Psi_\theta | \hat{H} | \Psi_\theta \rangle}{\langle \Psi_\theta | \Psi_\theta \rangle} = \sum_i \frac{|\langle D_i | \Psi_\theta \rangle|^2}{\sum_k |\langle D_k | \Psi_\theta \rangle|^2} E_{loc}(D_i), \quad (3)$$

where we have defined the local energy

$$E_{loc}(D_i) = \frac{\langle D_i | \hat{H} | \Psi_\theta \rangle}{\langle D_i | \Psi_\theta \rangle} = \sum_\mu \langle D_i | \hat{H} | D_\mu \rangle \frac{\langle D_\mu | \Psi_\theta \rangle}{\langle D_i | \Psi_\theta \rangle}. \quad (4)$$

To circumvent the summation over the full configuration space in eq 3, the MC method gives an unbiased estimation of the energy by $E_\theta = \langle E_{loc}(D_i) \rangle_{P_i}$, which averages the local energy over a configuration sample V drawn from the probability distribution $P_i = \frac{|\langle D_i | \Psi_\theta \rangle|^2}{\sum_k |\langle D_k | \Psi_\theta \rangle|^2}$. The MC procedure for generating this configuration sample V utilizes $|\langle D_i | \Psi_\theta \rangle|^2$ only and realizes a Markov chain $|D\rangle_0 \rightarrow |D\rangle_1 \rightarrow |D\rangle_2 \rightarrow \dots$ by performing random walks according to the Metropolis-Hastings algorithm⁴⁸. Configurations on the Markov chain then constitute the MC sample V , which generally contains N_{tot} configurations and can be represented by N_{unique} unduplicated configurations $\{|D_i\rangle\}$ with their repetitions N_i . Thus, the inaccessible accurate probability P_i can be estimated by statistical probability $P_i \approx \frac{N_i}{N_{tot}}$, where $N_{tot} = \sum_{i=1}^{N_{unique}} N_i$, and the energy of NQS can then be calculated through

$$E_\theta \approx \sum_{i \in V} \frac{N_i}{N_{tot}} E_{loc}(D_i). \quad (5)$$

Furthermore, the MC method makes it possible to minimize the energy of NQS with respect to its parameters θ by utilizing iterative gradient-based algorithms, as this would optimize NQS to the ground state wave functions according to the variational principle. Due to the energy E_θ is a real-valued function with complex-valued parameters, the negative of the gradient with respect to the conjugate of the neural-network parameters defines the direction of the steepest descent according to Wirtinger calculus⁴⁹. This can be evaluated as

$$g_{\theta_k} = \frac{\partial E_\theta}{\partial \theta_k^*} = \frac{\langle \Psi'_{\theta_k} | \hat{H} | \Psi_\theta \rangle}{\langle \Psi_\theta | \Psi_\theta \rangle} - E_\theta \frac{\langle \Psi'_{\theta_k} | \Psi_\theta \rangle}{\langle \Psi_\theta | \Psi_\theta \rangle}, \quad (6)$$

where $|\Psi'_{\theta_k}\rangle = \sum_i \frac{\partial \langle D_i | \Psi_\theta \rangle}{\partial \theta_k} \times |D_i\rangle$. It is worth noting that this complicated formula can also be estimated using the MC sample V that obtained when calculating the energy, i.e.,

$$g_{\theta_k} = \langle O_{i\theta_k}^* E_{loc}(D_i) \rangle_{P_i} - E_{\theta} \langle O_{i\theta_k}^* \rangle_{P_i}, \quad (7)$$

where $O_{i\theta_k} = \frac{\partial \ln \langle D_i | \Psi_{\theta} \rangle}{\partial \theta_k}$.

Finally, the stochastic reconfiguration (SR) scheme⁵⁰, a second-order method which can be viewed as an approximate imaginary time evolution in the variational subspace, is used to ensure a more rapid and robust convergence compared to the first-order stochastic gradient descent (SGD) method. In the SR algorithm, the parameter update $\Delta\theta$ is given by the linear equation

$$S_{mn} \Delta\theta = -\eta g_{\theta}, \quad (8)$$

where $S_{mn} = \langle O_{i\theta_m}^* O_{i\theta_n} \rangle_{P_i} - \langle O_{i\theta_m}^* \rangle_{P_i} \langle O_{i\theta_n} \rangle_{P_i} + \lambda \cdot \delta_{mn}$, η is the step size and λ is a regularization parameter that stabilizes optimization. Generally, the parameter update $\Delta\theta$ would rotate towards the steepest decent direction as the λ becomes larger^{51, 52}. The step size η is another significant hyperparameter and an adaptive algorithm⁵³ can be used to automatically adjust it during the optimization.

3. ALGORITHMIC IMPROVEMENTS

3.1. Deterministic Selection in Configuration Space. Despite the success of MC sampling in optimizing NQS, it also leads to several challenges when applying the NQS to chemical systems. In molecular systems the configuration probabilities span many orders of magnitudes and peaks around the Hartree-Fock and neighboring excited states, as is one common peculiarity of the ground-state wave functions in quantum chemistry, thus the standard uniform MC sampling often fails to efficiently sample those less likely but chemically relevant configurations. Besides, the MC sampling also introduces statistical instability to the NQS optimization, which is observed from the change of energy or configuration coefficients over iterations and able to be reduced via using deterministically generated samples instead²⁵. Therefore, an alternative method to efficiently and deterministically generate the configuration sample V that contains most of the chemically important configurations is helpful.

Here we found that the iterative construction schemes of SCI methods can be adapted to build such a configuration sample V during the optimization of NQS with efficiency. In typical SCI methods¹⁵, the full configuration space is divided into three parts: the core space V_{core} with all selected significant configurations or determinants, the connected space V_{conn} containing all other

configurations connected to the current core space by Hamiltonian matrix elements that have a nonzero or sufficiently large amplitude, and the rest of the configuration space. The SCI methods then iteratively select out important configurations from V_{conn} , using perturbation theory, and add them into V_{core} . Likewise, in the optimization of NQS, the required configuration sample V is the equivalent of the core space V_{core} , and its connected space V_{conn} is generated naturally when calculating the energy of NQS. Therefore, when optimizing the NQS, we can similarly select out important configurations from V_{conn} , using the modulus of NQS ansatz instead, and update the configuration sample V at each iteration. In details, starting from the configuration sample $V = \{|D_i\rangle\}$ obtained in last iteration, we deterministically update this sample V with NQS ansatz $|\Psi_\theta\rangle$ as follows:

- (1) **Calculate local energy of each configuration in current sample V as required by NQS optimization and simultaneously select out important configurations from its connected space.** When calculating the local energy $E_{loc}(D_i) = \sum_\mu \langle D_i | \hat{H} | D_\mu \rangle \frac{\langle D_\mu | \Psi_\theta \rangle}{\langle D_i | \Psi_\theta \rangle}$ of each configuration $|D_i\rangle$ in sample V , all of the configurations that denoted by $|D_\mu\rangle$ and treated with the evaluation of their coefficients $\langle D_\mu | \Psi_\theta \rangle$ compose exactly the connected space of sample V , thus we can select out those important configurations in connected space under condition of $|\langle D_\mu | \Psi_\theta \rangle| > \epsilon$ along with the energy calculation. Here the NQS ansatz is an intermediate normalized form with the largest $|\langle D_i | \Psi_\theta \rangle|$ in sample V set to be one, and $|D_\mu\rangle$ that has been contained in sample V is discarded.
- (2) **Update the sample V with these deterministically selected important configurations.** First remove configurations that do not satisfy $|\langle D_i | \Psi_\theta \rangle| > \epsilon$ in the current sample V , and then merge the rest of the sample V with these selected configurations.

During the iterative optimization of NQS, the initial configuration sample V is one MC sample and will be deterministically updated at each iteration. In general, the updated sample V continuously contains all desired configurations that satisfy $|\langle D_i | \Psi_\theta \rangle| > \epsilon$ after the initial few iterations, and the size of sample V can be conveniently adjusted through the magnitude of ϵ . In the limit that $\epsilon = 0$, the full configuration space is selected. It is fair to say that, for example, an exact selection with $\epsilon = 10^{-6}$ is similar to a MC sampling of square modulus with 10^{12} total configurations but without noise.

3.2. Non-stochastic Optimization of NQS. Here we introduce how to apply the deterministic selection scheme in configuration space to the optimization of NQS. As mentioned in Section 2.2,

the accurate probability $P_i = \frac{|\langle D_i | \Psi_\theta \rangle|^2}{\sum_k |\langle D_k | \Psi_\theta \rangle|^2}$ of each configuration is required to evaluate the energy of NQS. Due to the intractable summation over full configuration space in the denominator of accurate P_i , one statistical approximation $P_i \approx \frac{N_i}{N_{tot}}$ based on MC sampling is usually applied when using a MC sample as shown in eq 5. However, if we use the deterministically selected sample, a new approximation that do not rely on MC sampling is required. Therefore, we proposed to use $P_i \approx \frac{|\langle D_i | \Psi_\theta \rangle|^2}{\sum_{k \in V} |\langle D_k | \Psi_\theta \rangle|^2}$, only counting those configurations that are included in the configuration sample V . This approximation can be also used with a MC sample and usually make sense because for these configurations outside the sample V , the terms $|\langle D_k | \Psi_\theta \rangle|^2$ in the summation are small enough to be omitted. Moreover, this new approximation is more accurate than $\frac{N_i}{N_{tot}}$, especially when N_{tot} is not big enough. With the new approximation, the energy expectation value of NQS can be derived as

$$E_\theta \approx \sum_{i \in V} \frac{|\langle D_i | \Psi_\theta \rangle|^2}{\sum_{k \in V} |\langle D_k | \Psi_\theta \rangle|^2} E_{loc}(D_i), \quad (9)$$

and the other expectation values can be estimated similarly.

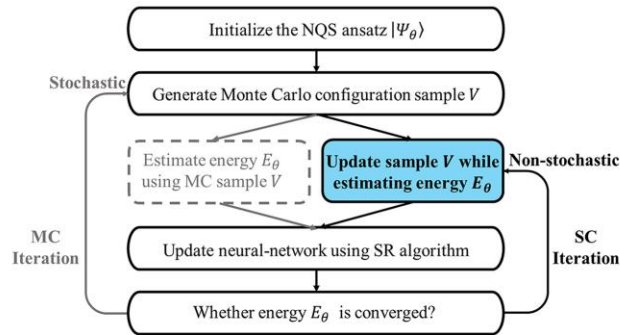


Figure 1. Schematic of two types of optimization scheme for NQS. In the third step, the gray block belongs to the stochastic MC iteration scheme while the blue block is part of the non-stochastic SC iteration scheme. The stochastic MC iteration scheme utilizes MC samples, thus requires MC sampling at each iteration. The non-stochastic SC iteration scheme utilizes selected configuration samples and updates the sample while estimating energy, thus avoids MC sampling at each iteration.

In order to exhibit the change of the whole optimization process after replacing the MC sample with the deterministically selected sample, we give the schematic of two types of optimization scheme for NQS in Figure 1. The most important difference between these two types of optimization scheme is that our newly developed non-stochastic *selected configuration* (SC) iteration scheme evades the time-consuming MC sampling in each iteration loop and combines the update of configuration sample V with the energy evaluation, which lead to an encouraging improvement on the speed of NQS optimization. Besides, this non-stochastic SC iteration scheme can also give a more stable optimization process than the stochastic MC iteration scheme.

The SC iteration scheme is thus supposed to result in a faster and more stable optimization of NQS as shown in Section 4.1. In practice, we can control the size of selected sample through adjusting the magnitude of ϵ in selection condition $|\langle D_i | \Psi_\theta \rangle| > \epsilon$. For large chemical systems, a larger value of ϵ is suggested in the initial iterations, because when optimizing one randomly initialized NQS ansatz in the initial few iterations, NQS ansatz far from the ground-state wave function usually results in very large selected configuration samples. Furthermore, we can also use the MC iteration scheme with limited sample size to pre-optimize the randomly initiated NQS ansatz, making the NQS ansatz resemble one real ground-state wave function and suitable to be optimized through the SC iteration scheme.

3.3. Perturbative Correction to the Variational Energy. Although the variational energy of NQS has been shown in some cases to be better than the coupled cluster with singles, doubles, and perturbative triples (CCSD(T)) method², the “gold standard” of quantum chemistry, we can still make efforts to go beyond the VMC framework and achieve the accuracy level of the most advanced quantum chemistry methods such as DMRG, SCI, and full configuration interaction quantum Monte Carlo⁵⁴⁻⁵⁶ (FCIQMC). One of the approaches to realize this is employing the perturbation theory.

One straight pathway to apply perturbation theory is similar to SCI+PT methods and is convenient for small active space. It is obvious that the deterministically selected configuration sample V generated at the final SC iteration with selection criterion ϵ is equivalent to the core space V_{core} constructed in SCI+PT methods, as both of them are collections of the most important configurations in the full configuration space. Therefore, a selected configuration interaction energy E_{SCI} can be obtained by calculating the lowest eigenvalue of the Hamiltonian in selected configuration sample V with eigenvector $|\Psi_{SCI}\rangle = \sum_{i \in V} c_i |D_i\rangle$. Moreover, an approximate second-order perturbative correction to the energy E_{SCI} can be given by

$$\Delta E^{(2)} \approx \sum_{k \in V_{conn}} \frac{(\sum_{i \in V} \langle D_k | \hat{H} | D_i \rangle c_i)^2}{E_{SCI} - \langle D_k | \hat{H} | D_k \rangle}, \quad (10)$$

which is the same as what is used in one of the SCI+PT methods, termed Heat-bath configuration interaction¹⁵ (HCI). The final energy $E_{SCI+PT} = E_{SCI} + \Delta E^{(2)}$ usually achieves a much higher accuracy than the variational energy E_θ and E_{SCI} .

Besides, another way to apply the perturbative theory was recently proposed to correct non-linearly parametrized wave functions, which eludes the diagonalization of the Hamiltonian in selected configuration sample and thus is efficient for large active space⁵⁷. We adapt this scheme by approximating the NQS wave function with $|\Psi_{NQS}\rangle \approx \sum_{i \in V} \langle D_i | \Psi_\theta \rangle \times |D_i\rangle$, where V is the selected configuration sample, and re-defining the local energy as $E(D_i) = \frac{\langle D_i | \hat{H} | \Psi_{NQS} \rangle}{\langle D_i | \Psi_{NQS} \rangle}$. Thus, the perturbatively corrected energy of NQS wave function can be derived as

$$E_{NQS+PT} = E_0 + \sum_{i \in V} \frac{|\langle D_i | \Psi_{NQS} \rangle|^2 |E(D_i) - E_0|^2}{\langle \Psi_{NQS} | \Psi_{NQS} \rangle (E_0 - H_{ii})} + \sum_{k \in V_{conn}} \frac{1}{\langle \Psi_{NQS} | \Psi_{NQS} \rangle} \frac{|\langle D_k | \hat{H} | \Psi_{NQS} \rangle|^2}{E_0 - H_{kk}}, \quad (11)$$

where $E_0 = \frac{\langle \Psi_{NQS} | \hat{H} | \Psi_{NQS} \rangle}{\langle \Psi_{NQS} | \Psi_{NQS} \rangle}$ and $H_{ii} = \langle D_i | \hat{H} | D_i \rangle$.

4. RESULTS

4.1. Comparison with Stochastic MC Iteration Scheme. We first compare the performance of the non-stochastic SC iteration scheme with the stochastic MC iteration scheme by calculating the ground state of carbon dimer at its equilibrium bond length of 1.26 Å in the minimal STO-3G basis set. We use the RBM ansatz with hidden unit density $\alpha = 2$ and fix the seed for random number generator to allow a fair comparison.

As shown in Figure 2a, these two iteration schemes exhibit the same behavior in large scale but behave much differently if we focus on the last hundreds of iterations. The non-stochastic SC iteration scheme drops the energy more smoothly and gives a lower converged energy in less iterations, while the stochastic MC iteration scheme gradually reduces energy with prominent oscillations and cannot converge in one thousand iterations. In addition, the non-stochastic SC iteration scheme can obtain more significant configurations during optimizations as expected. Specifically, when using the same optimized RBM wave function, the SC iteration scheme deterministically selected 3,910 unique configurations with the criterion $|\langle D_i | \Psi_\theta \rangle| > 10^{-6}$

while the stochastic MC iteration scheme sampled only 509 unique configurations with $N_{tot} = 10^6$. A better accuracy than CCSD(T) method is also achieved using the non-stochastic SC iteration scheme. Its converged ground-state energy $E_{RBM} = -74.6891$ Ha is about 1.5 mHa lower than $E_{CCSD(T)} = -74.6876$ Ha and around 1.7 mHa higher than $E_{FCI} = -74.6908$ Ha. This is in agreement with the value -74.6892 Ha obtained from the first application of RBM ansatz to C_2 molecule²⁴, which could also be achieved in our experiment by changing the convergence criterion and optimizing another 170 iterations.

The improved speed when using the non-stochastic SC iteration scheme is another highlight of this approach, which can be clearly explained by the evasion of the time-consuming MC sampling. Meanwhile, deterministically updating selected configuration sample along with energy evaluation requires negligible extra effort. We can see in Figure 2b that the computational cost over iterations of the stochastic MC iteration scheme is much steeper than that of the non-stochastic SC iteration scheme. Before the turning point at the 58th iteration, we use the MC iteration scheme to pre-optimize the RBM ansatz, and then start the SC iteration scheme as the expectation energy of RBM ansatz has been lower than the corresponding Hartree-Fock energy. Roughly speaking, the SC iteration scheme takes only one eighth of the time that the MC iteration scheme costs in this case, and it could do better when the MC sampling becomes more time-consuming due to a larger neural network or a larger Monte Carlo sample.

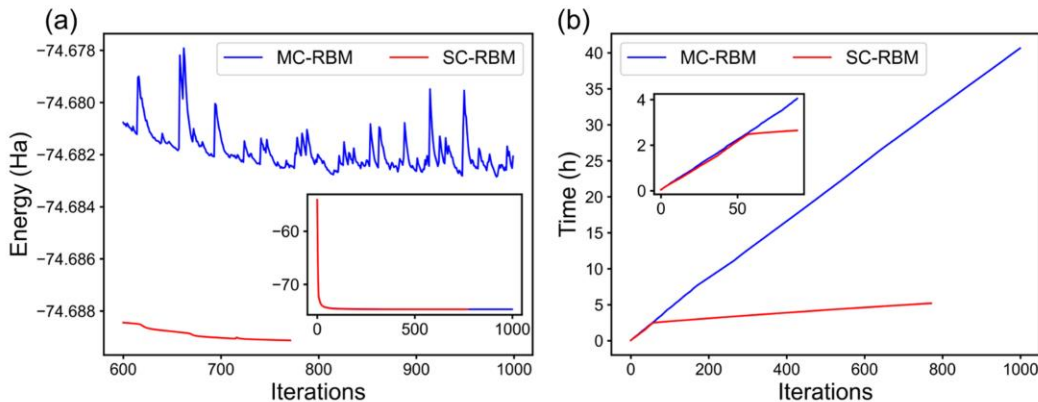


Figure 2. The performance of two types of optimization scheme for C_2 molecule at its equilibrium bond length of 1.26 Å in the minimal STO-3G basis set. MC-RBM is the stochastic MC iteration scheme, and SC-RBM is the non-stochastic SC iteration scheme. (a) Demonstration of the energy training process. (b) Wall time cost on 8 CPU cores over iterations.

4.2. Potential Energy Curve of Carbon Dimer. In this section, the performances of the non-stochastic SC iteration scheme and the perturbative correction are studied by calculating the

potential energy curves of ground-state carbon dimer with RBM ansatz in both the minimal STO-3G basis set and the larger cc-pVDZ basis set, as this diatomic molecule possesses strong correlations and multireference characteristics.

In the minimal STO-3G basis, the full variational space consists of 44,100 configurations and the number of important configurations selected in SC iterations with $\epsilon = 10^{-6}$ ranges from 2,500 to 7,000. We find that the SC iteration scheme also outperforms the standard quantum chemical method CCSD(T) as shown in Figure 3a and Table 1, which is in common with the MC iteration scheme²⁴. Furthermore, to detailedly show the capability of RBM ansatz in this system, we use four RBM ansatzes with different hidden unit density for comparison and give their energy deviations relative to FCI results in Figure 3b. It is obvious that the RBM ansatz with insufficient hidden units ($\alpha = 1$) has much poorer performances while other three RBM ansatzes usually give better results than CCSD(T) method. In particular, higher accuracy could be achieved by RBM ansatz with more hidden units in this case. However, no significant performance improvements are made by solely increasing the hidden unit density from 2 to 8, because of the difficulty in escaping local minima with more neural-network parameters. This supports a general rule that enough hidden units for RBM ansatz are required to capture correlation effects accurately, but simply adding more hidden units cannot always guarantee a performance boost in practice.

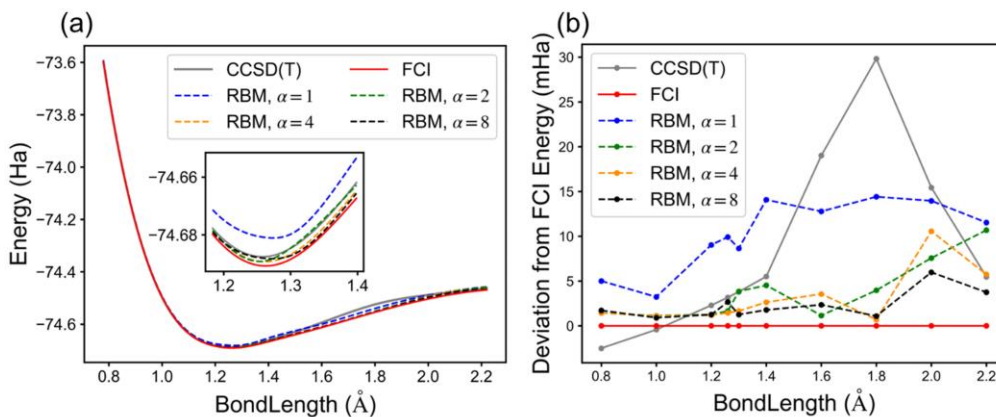


Figure 3. (a) Potential energy curves of C_2 in the minimal STO-3G basis set obtained through various approaches. (b) Difference between the FCI results and the energies using four RBM ansatzes with different hidden unit density α for C_2 at various bond lengths in the minimal STO-3G basis set.

Perturbative correction is applied to the optimized RBM wave function with $\alpha = 8$ by calculating E_{SCI} and E_{SCI+PT} with deterministically selected configuration sample in the last iteration of SC scheme. Table 1 shows the detailed energy errors of different methods. It is clear

that $E_{SCI+PT} < E_{SCI} < E_{\theta}$ is always obeyed in this case. The impressive aspect of this calculation is that the energy errors are reduced to 0.001~0.2 mHa after the perturbative correction. This successful application of the perturbation theory also demonstrates that the optimized RBM wave function can accurately identify chemically important configurations, which is similar to the agent in reinforcement learning configuration interaction⁵⁸.

Table 1. Energy errors relative to FCI results (in mHa) of a variety of methods for C₂ at various bond lengths (in Å) using the minimal STO-3G basis set.

Bond Length	CCSD(T)	RBM ($\alpha = 8$)	RBM-SCI	RBM-SCI+PT
0.80	-2.50	1.72	0.49	0.00
1.00	-0.43	0.90	0.30	0.00
1.20	2.29	1.26	0.53	0.01
1.26	3.17	2.65	0.92	0.04
1.30	3.80	1.26	0.25	0.00
1.40	5.51	1.77	0.32	0.01
1.60	19.01	2.35	0.31	0.01
1.80	29.82	1.08	0.19	0.01
2.00	15.44	5.98	1.00	0.07
2.20	5.47	3.75	1.18	0.19

In the cc-pVDZ basis, we use the natural orbitals from CAS(8e,14o) calculations because they are supposed to be more appropriate to describe the multireference carbon dimer than canonical Hartree-Fock orbitals. When optimizing the RBM ansatz, all 12 electrons were fully correlated in 28 molecular orbitals without symmetry. The full variational space consists of $\sim 1.4 \times 10^{11}$ configurations and tens of thousands of important configurations are selected in SC iterations with $\epsilon = 10^{-6}$. We can see in Figure 4 that the potential energy curve obtained from RBM wave function achieves an accuracy better than the CCSD results and shows a good relative energy to the FCI results⁵⁹ with correct prediction of local minimum. The average energy error is about 20 milihartrees and higher than the result in minimal STO-3G basis, because it is much harder for RBM ansatz to correctly fit the probability distribution in a larger configuration space.

Notably, the perturbatively corrected energy E_{RBM+PT} using eq 11 is lower than the CCSD(T) results and matches the FCI energy very well at short bond length, though differences can be

noticed when the bond is stretched. This is because that the accuracy of perturbation theory depends not only on the quality of RBM wave function but also the strength of electronic correlation. To further upgrade the performance of RBM wave function in this large chemical system, representability of RBM ansatz is a vital factor. However, due to the memory limit when utilizing the second-order SR algorithm, hidden unit density of the RBM ansatz used here is just two, which is probably not enough for such a large configuration space. Therefore, it is crucial to explore other possible NQS architectures that possess higher representational capacity to treat chemical systems and it is also worth searching other parameter optimization algorithms that require less memory and can efficiently escape local minimums of NQS.

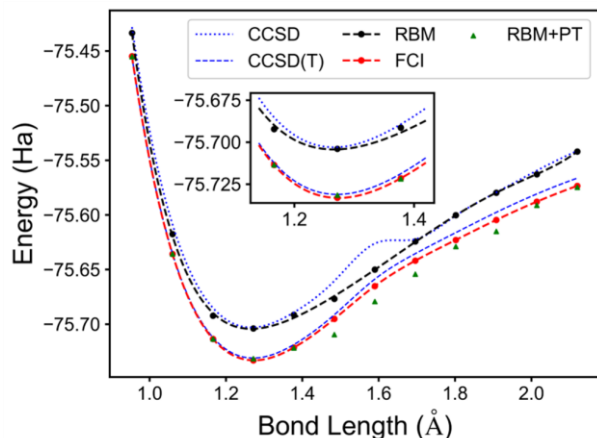


Figure 4. Potential energy curves of C_2 in the cc-pVDZ basis set. The variational energies of RBM ansatz and their perturbatively corrected energies (RBM+PT) are compared with the results of both FCI and coupled cluster methods (CCSD, CCSD(T)). The discontinuity in the energies of the CCSD method around 1.6 Å is because of a curve crossing between $^1\Sigma_g^+$ and $^1\Delta_g$ states⁵⁹.

4.3. Potential Energy Curve of Equidistant Linear Hydrogen Chain H_{10} . The linear chain of 10 equidistant hydrogen atoms is characterized by the distance between two adjacent atoms and has been recently studied to test various quantum chemical methods⁶⁰. In the minimal STO-6G basis set, H_{10} resembles a one-dimensional Hubbard model as there is only one orbital per hydrogen atom and exhibits stronger correlation compared to the carbon dimer studied above. From the quantum chemical perspective⁶¹, H_{10} is an elongated molecule in which the localized molecular orbital basis (LMO), such as the one obtained with the Boys-localization⁶² in PySCF packages^{63, 64}, is more appropriate than the canonical Hartree-Fock molecular orbital basis (CMO). Thus, H_{10} is a convenient system to manifest the different performance of NQS with LMOs and CMOs, as the

NQS wave function is always only an approximation to the real FCI wave function and is not invariant to orbital rotations.

As shown in Figure 5, the potential energy curve obtained by NQS wave function with LMOs matches the FCI curve very well throughout the whole dissociation curve, and it gives impressively small energy errors lower than 0.2 mHa . Nevertheless, deviations from the FCI curve at large H-H distance can be noticed when CMOs are used. It is shown in Figure 5b that the energy errors with CMOs can reach dozens of milihartrees and remain about 20 milihartrees at the last four points even if corrected by the perturbation theory.

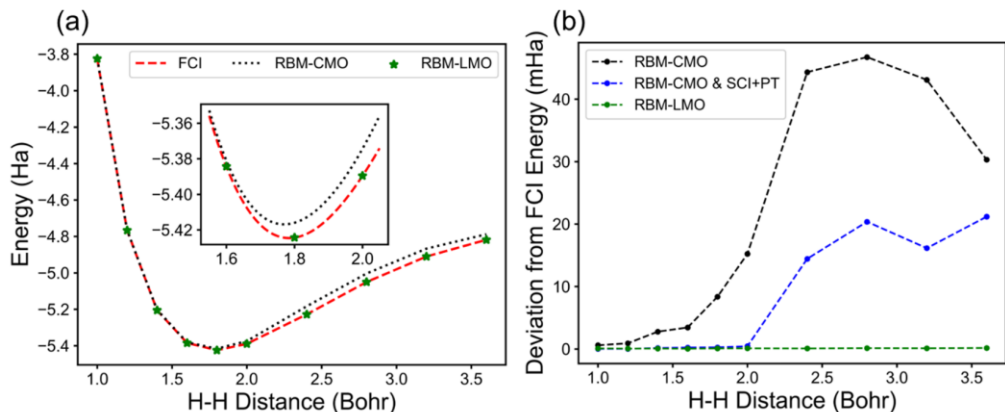


Figure 5. (a) Potential energy curves of linear hydrogen chain H_{10} in the minimal STO-6G basis set. The accuracy of RBM ansatz using CMOs or LMOs is compared with FCI results. (b) Deviations relative to the FCI results are shown here. The black and green lines indicate the variational energies obtained by RBM ansatz with CMOs and LMOs, and the blue line indicates the perturbatively corrected energies with CMOs. For all these calculations, the hidden unit density of RBM ansatz is four.

The beneficial result of using LMOs in the optimization of NQS wave function for H_{10} molecule is also present in DMRG calculations of such elongated molecules⁶⁵. The reason for this superiority of LMOs in NQS optimization is possibly that the configuration possibility distribution of H_{10} is a highly concentrated structure when using CMOs but a smoother structure when using LMOs. This is indicated by the number of selected configurations during the SC iteration scheme with the same criterion $|\langle D_i | \Psi_\theta \rangle| > 10^{-8}$, which ranges from 3,000 to 20,000 with CMOs and is about 60,000 with LMOs. Therefore, it is probably that the NQS wave function can fit the smoother structure more accurately, even though a larger number of selected configurations may require more hidden units. Overall, the very different behaviors of LMOs and CMOs in NQS wave function when handling H_{10} molecule illustrate that the form of molecular orbitals plays an important role

during the optimization of NQS wave function, and it is well worth optimizing molecular orbitals along with neural-network parameters in the future.

5. CONCLUSION

In this work, we have introduced a non-stochastic optimization algorithm for neural-network quantum states relying on a general exact selection scheme according to the modulus of NQS, which deterministically updates the sample of important configurations along with the energy evaluation and demands trivial extra cost. Meanwhile, we instead use the square modulus of NQS to approximate the probability of each configuration. We then test the non-stochastic optimization algorithm by applying it to the calculation of ab initio potential energy curves of carbon dimer in both STO-3G and cc-pVDZ basis and linear hydrogen chain H_{10} in STO-6G basis with RBM-based NQS. These successful applications suggest that our non-stochastic optimization algorithm is able to circumvent the inefficiency and noise of MC sampling in RBM-based NQS optimization. In principle this would keep true no matter what the neural-network architecture is. Furthermore, we utilize the perturbation theory with two different protocols to correct the variational energy of NQS ansatz after network optimization, which elevates the accuracy to be competitive with CCSD(T) method for carbon dimer in the large cc-pVDZ basis with a full variational space of $\sim 1.4 \times 10^{11}$ configurations.

Besides, different behaviors of NQS under orbital rotations are observed in H_{10} systems, indicating that to further upgrade the performance of NQS, it is worthwhile and practicable to incorporate the optimization of the Slater determinants, or equivalently the molecular orbitals into the optimization of NQS⁶⁶. This will enhance the numerical flexibility of NQS and make it more efficient to find the optimal ground-state energy in strongly correlated systems. Meanwhile, exploring other powerful neural-network architectures⁶⁷ or gradient-based parameter optimization algorithms⁶⁸ would also be helpful.

Corresponding Author

*E-mail: hshu@mail.tsinghua.edu.cn.

ACKNOWLEDGMENT

This work was financially supported by the National Natural Science Foundation of China (Grant Nos. 22222605 and 22076095) and the Tsinghua Xuetao Talents Program. Mr. Xiang Li thanks Dr. Junjie Song of Tsinghua University for helpful discussions.

REFERENCES

- (1) Purvis, G. D.; Bartlett, R. J., A full coupled-cluster singles and doubles model: The inclusion of disconnected triples. *J. Chem. Phys.* **1982**, *76* (4), 1910-1918.
- (2) Raghavachari, K.; Trucks, G. W.; Pople, J. A.; Head-Gordon, M., A fifth-order perturbation comparison of electron correlation theories. *Chemical Physics Letters* **1989**, *157* (6), 479-483.
- (3) Per, S.; Anders, H.; Björn, R.; Bernard, L., A Comparison of the Super-CI and the Newton-Raphson Scheme in the Complete Active Space SCF Method. *Phys. Scr.* **1980**, *21* (3-4), 323.
- (4) Andersson, K.; Malmqvist, P. A.; Roos, B. O.; Sadlej, A. J.; Wolinski, K., Second-order perturbation theory with a CASSCF reference function. *The Journal of Physical Chemistry* **1990**, *94* (14), 5483-5488.
- (5) Werner, H. J.; Knowles, P. J., An efficient internally contracted multiconfiguration-reference configuration interaction method. *J. Chem. Phys.* **1988**, *89* (9), 5803-5814.
- (6) Lyakh, D. I.; Musiał, M.; Lotrich, V. F.; Bartlett, R. J., Multireference Nature of Chemistry: The Coupled-Cluster View. *Chem. Rev.* **2012**, *112* (1), 182-243.
- (7) Baiardi, A.; Reiher, M., The density matrix renormalization group in chemistry and molecular physics: Recent developments and new challenges. *J. Chem. Phys.* **2020**, *152* (4), 040903.
- (8) Schollwöck, U., The density-matrix renormalization group in the age of matrix product states. *Ann. Phys.* **2011**, *326* (1), 96-192.
- (9) Orús, R., A practical introduction to tensor networks: Matrix product states and projected entangled pair states. *Ann. Phys.* **2014**, *349*, 117-158.
- (10) Li, Z., Expressibility of comb tensor network states (CTNS) for the P-cluster and the FeMo-cofactor of nitrogenase. *Electron. Struct.* **2021**, *3* (1), 014001.
- (11) Huron, B.; Malrieu, J. P.; Rancurel, P., Iterative perturbation calculations of ground and excited state energies from multiconfigurational zeroth-order wavefunctions. *J. Chem. Phys.* **1973**, *58* (12), 5745-5759.
- (12) Liu, W.; Hoffmann, M. R., iCI: Iterative CI toward full CI. *J. Chem. Theory Comput.* **2016**, *12* (3), 1169-1178.
- (13) Tubman, N. M.; Lee, J.; Takeshita, T. Y.; Head-Gordon, M.; Whaley, K. B., A deterministic alternative to the full configuration interaction quantum Monte Carlo method. *J. Chem. Phys.* **2016**, *145* (4), 044112.

- (14) Schriber, J. B.; Evangelista, F. A., Communication: An adaptive configuration interaction approach for strongly correlated electrons with tunable accuracy. *J. Chem. Phys.* **2016**, *144* (16), 161106.
- (15) Holmes, A. A.; Tubman, N. M.; Umrigar, C. J., Heat-Bath Configuration Interaction: An Efficient Selected Configuration Interaction Algorithm Inspired by Heat-Bath Sampling. *J. Chem. Theory Comput.* **2016**, *12* (8), 3674-3680.
- (16) Sharma, S.; Holmes, A. A.; Jeanmairet, G.; Alavi, A.; Umrigar, C. J., Semistochastic Heat-Bath Configuration Interaction Method: Selected Configuration Interaction with Semistochastic Perturbation Theory. *J. Chem. Theory Comput.* **2017**, *13* (4), 1595-1604.
- (17) Coe, J. P., Machine Learning Configuration Interaction. *J. Chem. Theory Comput.* **2018**, *14* (11), 5739-5749.
- (18) Coe, J. P., Machine Learning Configuration Interaction for ab Initio Potential Energy Curves. *J. Chem. Theory Comput.* **2019**, *15* (11), 6179-6189.
- (19) Zhang, N.; Liu, W.; Hoffmann, M. R., Iterative Configuration Interaction with Selection. *J. Chem. Theory Comput.* **2020**, *16* (4), 2296-2316.
- (20) Epstein, P. S., The Stark Effect from the Point of View of Schroedinger's Quantum Theory. *Physical Review* **1926**, *28* (4), 695-710.
- (21) Nesbet, R. K.; Hartree, D. R., Configuration interaction in orbital theories. *Proceedings of the Royal Society of London. Series A. Mathematical and Physical Sciences* **1955**, *230* (1182), 312-321.
- (22) Freericks, J. K.; Nikolić, B. K.; Frieder, O., The nonequilibrium quantum many-body problem as a paradigm for extreme data science. *International Journal of Modern Physics B* **2014**, *28* (31), 1430021.
- (23) Carleo, G.; Troyer, M., Solving the quantum many-body problem with artificial neural networks. *Science* **2017**, *355* (6325), 602-606.
- (24) Choo, K.; Mezzacapo, A.; Carleo, G., Fermionic neural-network states for ab-initio electronic structure. *Nat. Commun.* **2020**, *11* (1), 2368.
- (25) Yang, P.-J.; Sugiyama, M.; Tsuda, K.; Yanai, T., Artificial Neural Networks Applied as Molecular Wave Function Solvers. *J. Chem. Theory Comput.* **2020**, *16* (6), 3513-3529.
- (26) Xia, R.; Kais, S., Quantum machine learning for electronic structure calculations. *Nat. Commun.* **2018**, *9* (1), 4195.
- (27) Torlai, G.; Mazzola, G.; Carleo, G.; Mezzacapo, A., Precise measurement of quantum observables with neural-network estimators. *Phys. Rev. Research* **2020**, *2* (2), 022060.
- (28) Han, J.; Zhang, L.; E, W., Solving many-electron Schrödinger equation using deep neural networks. *Journal of Computational Physics* **2019**, *399*, 108929.
- (29) Hermann, J.; Schätzle, Z.; Noé, F., Deep-neural-network solution of the electronic Schrödinger equation. *Nat. Chem.* **2020**, *12* (10), 891-897.
- (30) Pfau, D.; Spencer, J. S.; Matthews, A. G. D. G.; Foulkes, W. M. C., Ab initio solution of the many-electron Schrödinger equation with deep neural networks. *Phys. Rev. Research* **2020**, *2* (3), 033429.
- (31) Hermann, J.; Spencer, J.; Choo, K.; Mezzacapo, A.; Foulkes, W. M. C.; Pfau, D.; Carleo, G.; Noé, F., Ab-initio quantum chemistry with neural-network wavefunctions. *arXiv preprint arXiv:2208.12590* **2022**.

- (32) Chen, J.; Cheng, S.; Xie, H.; Wang, L.; Xiang, T., Equivalence of restricted Boltzmann machines and tensor network states. *Phys. Rev. B* **2018**, *97* (8), 085104.
- (33) Glasser, I.; Pancotti, N.; August, M.; Rodriguez, I. D.; Cirac, J. I., Neural-Network Quantum States, String-Bond States, and Chiral Topological States. *Physical Review X* **2018**, *8* (1), 011006.
- (34) Li, S.; Pan, F.; Zhou, P.; Zhang, P., Boltzmann machines as two-dimensional tensor networks. *Phys. Rev. B* **2021**, *104* (7), 075154.
- (35) Gao, X.; Duan, L.-M., Efficient representation of quantum many-body states with deep neural networks. *Nat. Commun.* **2017**, *8* (1), 662.
- (36) Nomura, Y.; Darmawan, A. S.; Yamaji, Y.; Imada, M., Restricted Boltzmann machine learning for solving strongly correlated quantum systems. *Phys. Rev. B* **2017**, *96* (20), 205152.
- (37) Carleo, G.; Nomura, Y.; Imada, M., Constructing exact representations of quantum many-body systems with deep neural networks. *Nat. Commun.* **2018**, *9* (1), 5322.
- (38) Sharir, O.; Levine, Y.; Wies, N.; Carleo, G.; Shashua, A., Deep Autoregressive Models for the Efficient Variational Simulation of Many-Body Quantum Systems. *Phys Rev Lett* **2020**, *124* (2), 020503.
- (39) Barrett, T. D.; Malyshev, A.; Lvovsky, A. I., Autoregressive neural-network wavefunctions for ab initio quantum chemistry. *Nature Machine Intelligence* **2022**, *4* (4), 351-358.
- (40) Zhao, T.; Stokes, J.; Veerapaneni, S., Scalable neural quantum states architecture for quantum chemistry. *arXiv preprint arXiv:2208.05637* **2022**.
- (41) Foulkes, W. M. C.; Mitas, L.; Needs, R. J.; Rajagopal, G., Quantum Monte Carlo simulations of solids. *Rev. Mod. Phys.* **2001**, *73* (1), 33-83.
- (42) Austin, B. M.; Zubarev, D. Y.; Lester, W. A., Quantum Monte Carlo and Related Approaches. *Chem. Rev.* **2012**, *112* (1), 263-288.
- (43) Deng, D.-L.; Li, X.; Das Sarma, S., Machine learning topological states. *Phys. Rev. B* **2017**, *96* (19), 195145.
- (44) Deng, D.-L.; Li, X.; Das Sarma, S., Quantum Entanglement in Neural Network States. *Physical Review X* **2017**, *7* (2), 021021.
- (45) Choo, K.; Carleo, G.; Regnault, N.; Neupert, T., Symmetries and Many-Body Excitations with Neural-Network Quantum States. *Phys Rev Lett* **2018**, *121* (16), 167204.
- (46) Vieijra, T.; Casert, C.; Nys, J.; De Neve, W.; Haegeman, J.; Ryckebusch, J.; Verstraete, F., Restricted Boltzmann Machines for Quantum States with Non-Abelian or Anyonic Symmetries. *Phys Rev Lett* **2020**, *124* (9), 097201.
- (47) Melko, R. G.; Carleo, G.; Carrasquilla, J.; Cirac, J. I., Restricted Boltzmann machines in quantum physics. *Nature Physics* **2019**, *15* (9), 887-892.
- (48) Hastings, W. K., Monte Carlo Sampling Methods Using Markov Chains and Their Applications. *Biometrika* **1970**, *57* (1), 97-109.
- (49) Zhang, H.; Mandic, D. P., Is a Complex-Valued Stepsize Advantageous in Complex-Valued Gradient Learning Algorithms? *IEEE Transactions on Neural Networks and Learning Systems* **2016**, *27* (12), 2730-2735.

- (50) Sorella, S.; Casula, M.; Rocca, D., Weak binding between two aromatic rings: Feeling the van der Waals attraction by quantum Monte Carlo methods. *J. Chem. Phys.* **2007**, *127* (1), 014105.
- (51) Toulouse, J.; Umrigar, C. J., Optimization of quantum Monte Carlo wave functions by energy minimization. *J. Chem. Phys.* **2007**, *126* (8), 084102.
- (52) Umrigar, C. J.; Toulouse, J.; Filippi, C.; Sorella, S.; Hennig, R. G., Alleviation of the Fermion-Sign Problem by Optimization of Many-Body Wave Functions. *Phys Rev Lett* **2007**, *98* (11), 110201.
- (53) Adams, C.; Carleo, G.; Lovato, A.; Rocco, N., Variational Monte Carlo Calculations of $A \leq 4$ Nuclei with an Artificial Neural-Network Correlator Ansatz. *Phys Rev Lett* **2021**, *127* (2), 022502.
- (54) Booth, G. H.; Thom, A. J. W.; Alavi, A., Fermion Monte Carlo without fixed nodes: A game of life, death, and annihilation in Slater determinant space. *J. Chem. Phys.* **2009**, *131* (5), 054106.
- (55) Cleland, D.; Booth, G. H.; Alavi, A., Communications: Survival of the fittest: Accelerating convergence in full configuration-interaction quantum Monte Carlo. *J. Chem. Phys.* **2010**, *132* (4), 041103.
- (56) Petruzielo, F. R.; Holmes, A. A.; Changlani, H. J.; Nightingale, M. P.; Umrigar, C. J., Semistochastic Projector Monte Carlo Method. *Phys Rev Lett* **2012**, *109* (23), 230201.
- (57) Sharma, S., Stochastic perturbation theory to correct non-linearly parametrized wavefunctions. *arXiv preprint arXiv:1803.04341* **2018**.
- (58) Goings, J. J.; Hu, H.; Yang, C.; Li, X., Reinforcement Learning Configuration Interaction. *J. Chem. Theory Comput.* **2021**, *17* (9), 5482-5491.
- (59) Sharma, S.; Alavi, A., Multireference linearized coupled cluster theory for strongly correlated systems using matrix product states. *J. Chem. Phys.* **2015**, *143* (10), 102815.
- (60) Simons Collaboration on the Many-Electron, P.; Motta, M.; Ceperley, D. M.; Chan, G. K.-L.; Gomez, J. A.; Gull, E.; Guo, S.; Jiménez-Hoyos, C. A.; Lan, T. N.; Li, J.; Ma, F.; Millis, A. J.; Prokof'ev, N. V.; Ray, U.; Scuseria, G. E.; Sorella, S.; Stoudenmire, E. M.; Sun, Q.; Tupitsyn, I. S.; White, S. R.; Zgid, D.; Zhang, S., Towards the Solution of the Many-Electron Problem in Real Materials: Equation of State of the Hydrogen Chain with State-of-the-Art Many-Body Methods. *Physical Review X* **2017**, *7* (3), 031059.
- (61) Guthrie, K.; Anderson, R. J.; Blunt, N. S.; Bogdanov, N. A.; Cleland, D.; Dattani, N.; Dobrautz, W.; Ghanem, K.; Jeszenszki, P.; Liebermann, N.; Manni, G. L.; Lozovoi, A. Y.; Luo, H.; Ma, D.; Merz, F.; Overy, C.; Rampp, M.; Samanta, P. K.; Schwarz, L. R.; Shepherd, J. J.; Smart, S. D.; Vitale, E.; Weser, O.; Booth, G. H.; Alavi, A., NECI: N-Electron Configuration Interaction with an emphasis on state-of-the-art stochastic methods. *J. Chem. Phys.* **2020**, *153* (3), 034107.
- (62) Foster, J. M.; Boys, S. F., Canonical Configurational Interaction Procedure. *Rev. Mod. Phys.* **1960**, *32* (2), 300-302.
- (63) Sun, Q.; Berkelbach, T. C.; Blunt, N. S.; Booth, G. H.; Guo, S.; Li, Z.; Liu, J.; McClain, J. D.; Sayfutyarova, E. R.; Sharma, S.; Wouters, S.; Chan, G. K.-L., PySCF: the Python-based simulations of chemistry framework. *WIREs Computational Molecular Science* **2018**, *8* (1), e1340.
- (64) Sun, Q.; Zhang, X.; Banerjee, S.; Bao, P.; Barbry, M.; Blunt, N. S.; Bogdanov, N. A.; Booth, G. H.; Chen, J.; Cui, Z.-H.; Eriksen, J. J.; Gao, Y.; Guo, S.; Hermann, J.; Hermes, M. R.; Koh, K.; Koval, P.; Lehtola, S.; Li, Z.; Liu, J.; Mardirossian, N.; McClain, J. D.; Motta, M.; Mussard, B.; Pham, H. Q.; Pulkin, A.; Purwanto, W.; Robinson, P. J.; Ronca, E.; Sayfutyarova, E. R.; Scheurer, M.; Schurkus, H. F.; Smith, J. E.

T.; Sun, C.; Sun, S.-N.; Upadhyay, S.; Wagner, L. K.; Wang, X.; White, A.; Whitfield, J. D.; Williamson, M. J.; Wouters, S.; Yang, J.; Yu, J. M.; Zhu, T.; Berkelbach, T. C.; Sharma, S.; Sokolov, A. Y.; Chan, G. K.-L., Recent developments in the PySCF program package. *J. Chem. Phys.* **2020**, *153* (2), 024109.

(65) Wouters, S.; Van Neck, D., The density matrix renormalization group for ab initio quantum chemistry. *The European Physical Journal D* **2014**, *68* (9), 272.

(66) Moreno, J. R.; Cohn, J.; Sels, D.; Motta, M., Enhancing the Expressivity of Variational Neural, and Hardware-Efficient Quantum States Through Orbital Rotations. *arXiv preprint arXiv:2302.11588* **2023**.

(67) von Glehn, I.; Spencer, J. S.; Pfau, D., A Self-Attention Ansatz for Ab-initio Quantum Chemistry. *arXiv preprint arXiv:2211.13672* **2022**.

(68) Martens, J.; Grosse, R., Optimizing neural networks with Kronecker-factored approximate curvature. In *Proceedings of the 32nd International Conference on International Conference on Machine Learning - Volume 37*, JMLR.org: Lille, France, 2015; pp 2408–2417.

Table of Contents

